International Journal of Advanced Engineering Research and Science (IJAERS)
Peer-Reviewed Journal
ISSN: 2349-6495(P) | 2456-1908(O)
Vol-11, Issue-2; Feb, 2024
Journal Home Page Available: https://ijaers.com/
Article DOI: https://dx.doi.org/10.22161/ijaers.112.6

Applying Weighted Taylor Series on Time Series Water Wave Modeling

Syawaluddin Hutahaean

Ocean Engineering Program, Faculty of Civil and Environmental Engineering,-Bandung Institute of Technology (ITB), Bandung 40132, Indonesia

Received: 22 Dec 2023,

Receive in revised form: 30 Jan 2024,

Accepted: 15 Feb 2024,

Available online: 26 Feb 2024

***Keywords*— weighted Taylor series, time series water wave model.**

***Abstract*—** *This study develops a time series model for water waves using a weighted Taylor series approach to analyze water wave dynamics. The model incorporates the continuity equation, Euler's momentum conservation equation, and the Kinematic Free Surface Boundary Condition, all formulated through the weighted Taylor series. By integrating the modified continuity equation across the water depth, utilizing depth-averaged velocity concepts, we derive the water surface elevation equation. Similarly, applying the Euler momentum conservation principle to the water surface yields an equation for the horizontal water particle velocity, which is subsequently converted into an expression for the horizontal depth-averaged velocity. The equations for water surface elevation and horizontal water particle velocity are solved using numerical methods. The application of the numerical model results in the generation of four distinct wave profiles: sinusoidal, Stokes, cnoidal, and solitary wave profiles, classified according to Wilson's (1963) criteria. The emergence of each wave profile type is influenced by the specified input wave height.*

I. INTRODUCTION

The Boussinesq equation, a cornerstone in the time series water wave model, has been developed in various forms by numerous researchers, including Boussinesq (1871), Dingermans (1997), Hamm, Madsen, and Peregrine (1993), Johnson (1997), Kirby (2003), and both the 1967 and 1972 works of Peregrine, among others. These versions encompass both the continuity and the water surface equations, as well as the water particle velocity equation. Each variant of the Boussinesq equation stems from the foundational principles of the continuity equation and Euler's momentum conservation equation, albeit with unique interpretations that lend each version its distinctive characteristics.

In our research, we developed a time series model that refines the basic hydrodynamic equations—the continuity equation and Euler's momentum conservation equation—through a weighted Taylor series approach. This method significantly minimizes, if not entirely eliminates, the truncation error typically associated with Taylor series approximations.

We derived the water surface elevation equation by integrating the continuity equation across the water depth, utilizing the concept of depth-averaged velocity. This integration employs the velocity potential equation from the solution to the Laplace equation for water particle velocity, ensuring precision in the integration process.

Furthermore, the horizontal water particle velocity equation was formulated by applying Euler's momentum conservation principle at the water surface. This equation was then converted into a horizontal depth-averaged velocity equation, leveraging the horizontal water particle equation from the velocity potential solution of the Laplace equation, thereby achieving exact transformation.

The core equations of our study—the surface water elevation equation and the horizontal depth-averaged water particle velocity equation—were solved numerically. The spatial differential was tackled using the Finite Difference Method, while the time differential was addressed through the predictor-corrector method. Both methods are characterized by second-order Taylor series accuracy, contingent upon the selection of an appropriately small grid size and time step to ensure the Taylor series is truncated to second-order differentials only. Our research calculated the grid size and time step to maintain the Taylor series truncation to first-order, aligning with the accuracy requirements of the Finite Difference Method.

Meticulous formulation of the basic hydrodynamic equations, governing equations, and numerical solutions, all executed with high precision will generate more reliable and accurate results.

II. WEIGHTED TAYLOR SERIES

Weighted Taylor series is a Taylor series that is truncated to only a first-order series, where the contribution of higher-order terms is expressed with coefficients called weighting coefficients (Hutahaean (2023a)).

For functions with two variables $f = f(x,t)$

$$f(x+\delta x, t+\delta t) = f(x,t) + \gamma_{t,2}\delta t\frac{\partial f}{\partial t} + \gamma_x \delta x \frac{\partial f}{\partial x} \quad \text{.....(1)}$$

$\gamma_{t,2}$ and γ_x are weighting coefficients.

For function $f = f(x,z,t)$ the weighted Taylor series is

$$f(x+\delta x, z+\delta z, t+\delta t) = f(x,z,t) + \gamma_{t,3}\delta t\frac{\partial f}{\partial t} + \gamma_x \delta x \frac{\partial f}{\partial x} + \gamma_z \delta z \frac{\partial f}{\partial z} \quad \text{.....(2)}$$

$\gamma_{t,3}$, γ_x and γ_z are weighting coefficients. There is no difference between γ_x in $f(x,t)$ and $\gamma_x$in f$((x,z,t)$. The basic values of the weighting coefficient are,

$\gamma_{t,2} = 2$; $\gamma_{t,3} = 3$; $\gamma_x = 1$; $\gamma_z = 1$

The foundational values in our model are obtained by eliminating higher-order even differential terms using the central difference method, a technique detailed by Hutahaean (2003a). The adjustments to weighting coefficients, addressing odd higher-order differential terms, are outlined in Table 1, where these coefficients are defined in relation to the optimization coefficient, ε. This relationship indicates that an increase in ε directly amplifies the impact of higher-order Taylor series terms on the analysis. Although the methodology for determining these coefficients is elaborated in Hutahaean (2023a), it is important to emphasize that the accuracy of the coefficients listed in Table 1 significantly exceeds those previously reported by Hutahaean (2023a), reflecting advancements in the precision of incorporating higher-order differential terms to enhance the model's predictive accuracy and reliability in hydrodynamic evaluations.

Table (1) Weighting coefficients.

ε	$\gamma_{t,2}$	$\gamma_{t,3}$	γ_x	γ_z
0.010	1.9998	3.0049	0.9988	1.0115
0.020	1.9992	3.0210	0.9951	1.0490
0.022	1.9990	3.0257	0.9941	1.0602
0.024	1.9988	3.0310	0.9930	1.0726
0.026	1.9986	3.0368	0.9918	1.0866
0.028	1.9984	3.0433	0.9904	1.1020
0.030	1.9981	3.0503	0.9890	1.1189
0.032	1.9979	3.0581	0.9875	1.1375
0.034	1.9976	3.0664	0.9858	1.1577
0.036	1.9973	3.0754	0.9841	1.1798
0.038	1.9970	3.0851	0.9823	1.2037
0.040	1.9966	3.0955	0.9803	1.2296

ε is the optimization coefficient, where in this time series model the selection of the weighting coefficient is determined by the wave amplitude the greater the wave amplitude the greater the ε, which is in the range of $0.015 < \varepsilon < 0.035$.

III. DEPTH INTEGRATION AND TRANSFORMATION COEFFICIENT

The formulation of the water surface equation is done by integrating the continuity equation with respect to water depth. The integration is carried out using the concept of depth average velocity (Dean (1991)) as follows.

$$U = \frac{1}{\beta_u D}\int_{-h}^{\eta} u\, dz \quad \text{.....(3)}$$

$U = U(x, z_0, t)$ is the horizontal particle depth average velocity, Fig (1)

z_0 is the elevation of U towards still water level.

$u = u(x,z,t)$ is the horizontal water particle velocity

β_u is integration coefficient

D is total water depth, $D = h + \eta$

h is water depth towards still water level

η is surface water elevation towards still water level

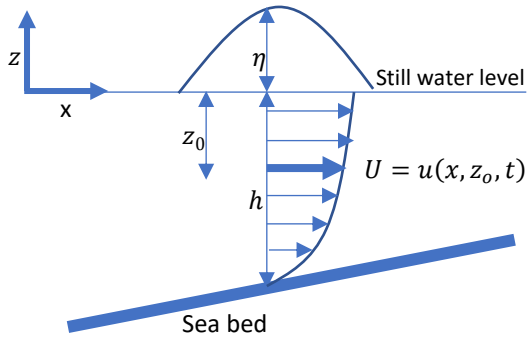

Fig (1). Depth average velocity concept

a. Integration coefficient β_u

In this study, a method for calculating the integration coefficient β_u was developed using the velocity potential equation and by establishing that the depth average velocity is $U = u(x, z_0, t)$, where the value of z_0 is determined (see Fig (1)).

Velocity potential solution of Laplace equation, at the characteristic point where $\cos kx = \sin kx$ (Hutahaean (2023b)) is,

$\phi(x, z, t) = 2G \cos kx \cosh k(h + z) \sin \sigma t$

$\phi(x, z, t)$ is potential velocity

G is wave constants

k is wave number

h is water depth towards still water level

σ is angular frequency

The horizontal velocity equation $u(x, z, t)$ is obtained using the velocity potential property:

$$u(x, z, t) = -\frac{\partial \phi}{\partial x}$$

$$u(x, z, t) = 2Gk \cos kx \cosh k(h + z) \sin \sigma t \quad \text{.....(4)}$$

It has been defined that the horizontal depth average velocity is the velocity at $z = z_0$ (Fig (1)), where z_0 is determined, then

$$U(x, z_0, t) = 2Gk \cos kx \cosh k(h + z_0) \sin \sigma t \quad \text{....(5)}$$

Employing (4) and (5),

$$\frac{u(x,z,t)}{U(x,z_0,t)} = \frac{\cosh k(h+z)}{\cosh k(h+z_0)} \quad \text{……(6)}$$

Equation (3) is written into the equation for the integration coefficient β_u,

$$\beta_u = \frac{1}{UD} \int_{-h}^{\eta} u \, dz$$

$$\beta_u = \frac{1}{D \cosh k(h + z_0)} \int_{-h}^{\eta} \cosh k(h + z) \, dz$$

Integration is completed,

$$\beta_u = \frac{\sinh k(h + \eta)}{kD \cosh k(h + z_0)}$$

$\eta = \frac{A}{2}$, A is wave amplitude, therefore

$$D = h + \frac{A}{2}$$

$$\beta_u = \frac{\sinh kD}{kD \cosh k(h + z_0)}$$

Hutahaean (2024) found that $kD = \theta\pi$ where $\tanh kD = \tanh \theta\pi \approx 1$, θ is the deep water coefficient, in this time series model research used $\theta = 1.80$. Determined $z_0 = -\xi h$, where $0 < \xi < 1$.. In deep water, $h \approx h + \frac{A}{2}$.

$$\beta_u = \frac{\sinh \theta\pi}{\theta\pi \cosh(\theta\pi(1-\xi))} \quad \text{……..(7)}$$

b. Transformation Coefficient $\alpha_{u\eta}$

In the process of integrating the continuity equation with respect to depth, there will be a horizontal surface water particle velocity u_η. This velocity must be transformed into the horizontal depth average velocity $U(x, z_0, t)$.

Using (4) and (5),

$$\frac{u_\eta}{U} = \frac{\cosh k\left(h + \frac{A}{2}\right)}{\cosh k(h + z_0)}$$

$$\frac{u_\eta}{U} = \frac{\cosh \theta\pi}{\cosh(\theta\pi(1 - \xi))}$$

Transformation coefficient $\alpha_{u\eta}$ is

$$\alpha_{u\eta} = \frac{\cosh \theta\pi}{\cosh(\theta\pi(1-\xi))} \quad \text{….(8)}$$

$$u_\eta = \alpha_{u\eta} U \quad \text{….(9)}$$

In the formulation of the equation for horizontal depth average velocity, the variable $u_\eta u_\eta$ must be transformed into U.

Using (4),

$u_\eta = 2Gk \cos kx \cosh k(h + \eta) \sin \sigma t$

$u_\eta u_\eta$ is mathematically expressed as

$u_\eta u_\eta = (2Gk \cos kx \cosh k(h + \eta) \sin \sigma t)^2$

However, since $u_\eta u_\eta$ moves simultaneously with u_η where the distribution of $u_\eta u_\eta$ according to space and time is the same as u_η, thus,

$u_\eta u_\eta = (2Gk)^2 \cos kx \cosh k(h + \eta) \sin \sigma t$

$UU = (2Gk)^2 \cos kx \cosh k(h + z_0) \sin \sigma t$

Therefore, the relation between $u_\eta u_\eta$ and UU is

$$u_\eta u_\eta = \alpha_{u\eta} UU \quad \text{……(10)}$$

As an illustration of the values of the integration coefficient β_u and the transformation coefficient $\alpha_{u\eta}$ can be seen in Table (2).

Table (2) The values of β_u and $\alpha_{u\eta}$

ξ	β_u	$\alpha_{u\eta}$
0.10	0.324	1.679
0.15	0.420	2.176
0.20	0.544	2.819
0.25	0.705	3.653

0.30	0.913	4.732
0.35	1.182	6.130
0.4	1.531	7.937

Table (2) shows that larger ξ is followed by deeper z_0, the larger the values of the integration coefficient β_u and the transformation coefficient $\alpha_{u\eta}$. In this study, a value of $\beta_u = 1$ was used, and using the Newton-Rhapson method, $\xi = 0.317612$ was obtained with a transformation coefficient value of $\alpha_{u\eta} = 5.183954$.

IV. WATER SURFACE ELEVATION EQUATION

4.1.Weighted continuity equation.

The continuity equation is formulated using the weighted Taylor series and by applying the principle of mass conservation,

$$\gamma_x \frac{\partial u}{\partial x} + \gamma_x \frac{\partial w}{\partial z} = 0 \qquad \ldots\ldots(11)$$

This equation is formulated under the condition that the horizontal particle velocity only changes along the horizontal axis, and similarly, the vertical particle velocity only changes along the vertical axis.

4.2. Integration of continuity equation

To obtain the water surface elevation equation, the continuity equation is integrated with respect to water depth, where the integration of the second term can be directly completed by ignoring the bottom vertical water particle velocity.

$$\int_{-h}^{\eta} \gamma_x \frac{\partial u}{\partial x} dz + \gamma_z w_\eta = 0$$

The vertical surface water particle velocity w_η is substituted with the Kinematic Free Surface Boundary Condition, where the weighted KFSBC (Hutahaean (2023a)) is as follows.

$$w_\eta = \gamma_{t,2} \frac{\partial \eta}{\partial t} + \gamma_x u_\eta \frac{\partial \eta}{\partial x}$$

Substituted into the integration of the continuity equation,

$$\int_{-h}^{\eta} \gamma_x \frac{\partial u}{\partial x} dz + \gamma_z \left(\gamma_{t,2} \frac{\partial \eta}{\partial t} + \gamma_x u_\eta \frac{\partial \eta}{\partial x} \right) = 0$$

The integration of the first term is solved by Leibniz integration (Protter, Murray, Morrey, & Charles, 1985),

$$\int_\alpha^\beta \frac{\partial f}{\partial x} dz = \frac{\partial}{\partial x} \int_\alpha^\beta f \, dz - f_\beta \frac{\partial \beta}{\partial x} + f_\alpha \frac{\partial \alpha}{\partial x} \qquad \ldots\ldots(12)$$

$$\int_{-h}^{\eta} \frac{\partial u}{\partial x} dz = \frac{\partial}{\partial x} \int_{-h}^{\eta} u \, dz - u_\eta \frac{\partial \eta}{\partial x} - u_{-h} \frac{\partial h}{\partial x}$$

The integration of the first term on the right side of the equation is completed using the concept of depth average velocity, and the horizontal bottom water particle velocity is ignored.

$$\int_{-h}^{\eta} \frac{\partial u}{\partial x} dz = \frac{\partial \beta_u UD}{\partial x} - u_\eta \frac{\partial \eta}{\partial x}$$

Substituted into the continuity equation integration, the surface velocity is transformed into depth average velocity, and the equation is written as the water surface equation,

$$\gamma_z \gamma_{t,2} \frac{\partial \eta}{\partial t} = -\gamma_x \beta_u \frac{\partial UD}{\partial x} + \gamma_x (1 - \gamma_z) \alpha_{u\eta} U \frac{\partial \eta}{\partial x}$$

$\ldots\ldots\ldots\ldots(13)$

(13) is the water surface elevation equation that is used to calculate the water surface elevation.

V. EULER'S MOMENTUM CONSERVATION EQUATION

By using the weighted Taylor series and the same fluid flow conditions as those used in the formulation of the continuity equation, where horizontal water particle velocity only changes along the horizontal axis and vertical water particle velocity only changes along the vertical axis, Euler's momentum conservation equation in the horizontal and vertical directions, respectively are presented as follows.

$$\frac{\partial u}{\partial t} + \gamma_x u \frac{\partial u}{\partial x} = -\frac{1}{\rho} \frac{\partial p}{\partial x} \qquad \ldots\ldots(14)$$

$$\frac{\partial w}{\partial t} + \gamma_z w \frac{\partial w}{\partial z} = -\frac{1}{\rho} \frac{\partial p}{\partial z} - g \qquad \ldots\ldots.(15)$$

Equation (15) is written as an equation for pressure p and integrated over water depth and the surface dynamic boundary condition $p_\eta = 0$ is performed

$$\frac{p}{\rho} = \gamma_{t,3} \int_z^{\eta} \frac{\partial w}{\partial t} dz + \frac{\gamma_z}{2} \left(w_\eta w_\eta - ww \right) + g(\eta - z)$$

Differentiated with respect to the x-horizontal axis,

$$\frac{1}{\rho} \frac{\partial p}{\partial x} = \gamma_{t,3} \frac{\partial}{\partial x} \int_z^{\eta} \frac{\partial w}{\partial t} dz + \frac{\gamma_z}{2} \frac{\partial}{\partial x} \left(w_\eta w_\eta - ww \right) + g \frac{\partial \eta}{\partial x}$$

Substituted to (14)

$$\gamma_{t,3} \frac{\partial u}{\partial t} + \frac{\gamma_x}{2} \frac{\partial uu}{\partial x} = -\gamma_{t,3} \frac{\partial}{\partial x} \int_z^{\eta} \frac{\partial w}{\partial t} dz - \frac{\gamma_z}{2} \frac{\partial}{\partial x} \left(w_\eta w_\eta - ww \right) - g \frac{\partial \eta}{\partial x}$$

This equation is worked out on the surface i.e. on $z = \eta$,

$$\gamma_{t,3} \frac{\partial u_\eta}{\partial t} + \frac{\gamma_x}{2} \frac{\partial u_\eta u_\eta}{\partial x} = -g \frac{\partial \eta}{\partial x}$$

The surface velocity is transformed into depth average velocity,

$$\gamma_{t,3} \alpha_{u\eta} \frac{\partial U}{\partial t} + \frac{\gamma_x \alpha_{u\eta}}{2} \frac{\partial UU}{\partial x} = -g \frac{\partial \eta}{\partial x} \qquad \ldots\ldots(16)$$

VI. VERTICAL WATER PARTICLE VELOCITY EQUATION

Both the water surface elevation equation and the horizontal water particle velocity do not include the variable of vertical water particle velocity. However, this velocity can be calculated in a simple manner, using the Kinematic Free Surface Boundary Condition:

$$w_\eta = \gamma_{t,2}\frac{\partial \eta}{\partial t} + u_\eta \frac{\partial \eta}{\partial t}$$

This surface velocity is transformed into depth average velocity.

$$W = \frac{1}{\alpha_{w\eta}}\left(\gamma_{t,2}\frac{\partial \eta}{\partial t} + \alpha_{u\eta} U \frac{\partial \eta}{\partial t}\right) \quad .....(17)$$

Where,

$$\alpha_{w\eta} = \frac{\sinh \theta\pi}{\sinh \theta\pi(1-\xi)} \quad .....(18)$$

Where θ and ξ are presented in Section 3.

VII. NUMERICAL SOLVING

Equations (13) and (16) are solved using numerical methods. The spatial differential is solved with the Finite Difference Method, and the time differential is solved using the predictor-corrector method.

7.1. Calculation of time step δt and grid size δx

Solving differential equations with numerical methods requires a specific time step and grid size to ensure good calculation results. The following section presents the equations for calculating these time steps and grid sizes. In principle, these equations are formulated based on the truncation of the Taylor series, which is the interval size where the Taylor series can be truncated to only a first-order series. The formulation of the equations can be seen in Hutahaean (2023a).

a. Time step δt calculation

Time step δt was measured using the following equation.

$$\frac{2}{3}\pi^2\varepsilon_t^2 - \pi\varepsilon_t + \varepsilon = 0 \quad ....(19)$$

ε is a small number that determines the size of the time step δt for example, $\varepsilon = 0.01$. The smaller the value of ε, the smaller ε_t and the smaller δt, where $\delta t = \varepsilon_t T$, T, with T being the wave period. In that equation, there are two values of ε_t; the smallest value is used.

b. Grid size δx measurement

The calculation of grid size δx requires the input time step δt obtained from (19). The equation to calculate δx is,

$$c_0 + c_1\varepsilon_x + c_2\varepsilon_x^2 = 0 \quad .....(20)$$

$$c_0 = 2\pi\varepsilon_t\varepsilon - 2\pi^2\varepsilon_t^2$$

$$c_1 = 2\pi\varepsilon + 4\pi^2\varepsilon_t$$

$$c_2 = -2\pi^2$$

There are two values of ε_x, the largest is used. Grid size $\delta x = \varepsilon_x L$,, where L is the wave length.

The formulations (19) and (20), with higher accuracy, can be seen in Hutahaean (2023a). However, the dominant factor determining accuracy is the choice of the value of ε. In principle, the smaller the value of ε. the better. In Table (3), the calculation results for δt and δx for waves with a wave period $T = 8.0$ sec, and a wave length $L = 16.0$ m are presented.

Table (3). Time step δt and grid size δx outcomes

ε	ε_t	ε_x	δt (sec.)	δx (m)
0.02	0.0065	0.0192	0.0516	0.3079
0.025	0.0081	0.0241	0.0648	0.3856
0.03	0.0097	0.029	0.078	0.4637
0.035	0.0114	0.0339	0.0913	0.542
0.04	0.0131	0.0388	0.1047	0.6207
0.045	0.0148	0.0437	0.1183	0.6997
0.05	0.0165	0.0487	0.1319	0.7791

As seen in Table (3), the larger the ε, the larger also the δt and δx. To check the compatibility between the time-step δt and the grid size δx, the Courant criterion (1928) is used as follows $\frac{\delta x}{\delta t} = 3\ C$

C adalah wave celerity dimana

$$C = \frac{\sigma}{k} = \frac{L}{T}\ m/sec$$

For example, for waves with a wave period $T = 8\ sec.$, and with a wave length $L = 16.0$ m, $C = 2.0\ m/sec$. The values of $\frac{\delta x/\delta t}{C}$ for δt and δx in Table (3) are calculated, with the calculation results presented in Table (4).

Table (4). Checking the Courant criteria

ε	δt (sec.)	δx (m)	$\delta x/\delta t$ (m/sec)	$\frac{\delta x/\delta t}{C}$
0.02	0.0516	0.3079	5.9639	2.982
0.025	0.0648	0.3856	5.9547	2.9774
0.03	0.078	0.4637	5.9454	2.9727
0.035	0.0913	0.542	5.9361	2.968
0.04	0.1047	0.6207	5.9267	2.9633
0.045	0.1183	0.6997	5.9172	2.9586
0.05	0.1319	0.7791	5.9076	2.9538

In Table (4), it is found that the values of δt and δx meet the Courant criterion, for all values of ε, which is ≈ 3.

Modeling in non-uniform water depths requires a non-uniform grid size as well. This is because different water depths have different wavelengths. In a non-uniform grid size, there is no difference or change in the Courant number.

$$\frac{\delta x}{\delta t} = \frac{\varepsilon_x}{\varepsilon_t}\frac{L}{T} = \frac{\varepsilon_x}{\varepsilon_t}C$$

The Courant number in this case is $\frac{\varepsilon_x}{\varepsilon_t}$. This value is constant for a given accuracy level ε, unaffected by wavelength or wave period. As an example, calculations for a sloping bottom with nonuniform wavelength are presented in Table (5), where a wave period of 8 sec is used, and the grid calculation uses $\varepsilon = 0.02$.

In Table (5), δt is constant, while δt is not, but the resulting Courant number,
is constant.

$$\frac{\delta x/\delta t}{C} = \frac{\varepsilon_x}{\varepsilon_t}$$

Table (5) Grid-size of non uniform water depth

L (m)	δt (sec.)	δx (m)	$\delta x/\delta t$ (m/sec)	$\frac{\delta x/\delta t}{C}$
16	0.05163	0.3079	5.9639	2.98195
14	0.05163	0.26941	5.21842	2.98195
12	0.05163	0.23093	4.47293	2.98195
10	0.05163	0.19244	3.72744	2.98195
8	0.05163	0.15395	2.98195	2.98195
6	0.05163	0.11546	2.23646	2.98195
4	0.05163	0.07698	1.49098	2.98195
2	0.05163	0.03849	0.74549	2.98195

The Finite Difference Method is formulated using a second-order Taylor series, where the Taylor series is truncated to second order only. Therefore, calculations with this method require small time steps and grid sizes. The time step and grid size calculated for the truncation of the first-order Taylor series definitely meet the requirements for the truncation of the second-order Taylor series.

c. Wave length measurement

For calculating grid size, information about the wave length is required. The following section discusses the method for calculating wave length.

The deep-water wave number is calculated using the equation,

$$\frac{gA_0}{2}k_0^2 - \frac{g\tanh(\theta\pi)}{\sqrt{\gamma_z}}k_0 + \gamma_{t,2}\gamma_{t,3}\sigma^2 = 0 \qquad \text{.....(21)}$$

g gravitational acceleration
A_0 deep water wave amplitude
$\sigma = \frac{2\pi}{T}$, T adalah wave period.
Deep water depth,

$$h_0 = \frac{\theta\pi}{k_0} - \frac{A_0}{2} \qquad \text{.....(22)}$$

Wave number of one water depth $h_x < h_0$,

$$k_x = \frac{k_0 h_0}{h_x}$$

Where wave length

$$L_x = \frac{2\pi}{k_x}$$

To conform to the wavelength model, in (21) the weighting coefficients are used: $\gamma_{t,2} = 1.8$, $\gamma_{t,2} = 2.6$, $\gamma_x = 1.0$ dan $\gamma_z = 1.0$.

7.2.Predictor-corrector method

When performing calculations with the finite difference method, a grid-points is established within the domain, using the grid size as previously discussed. At a given point i on the grid, the water surface elevation equation and horizontal water particle velocity can be rewritten as follows:

$$\frac{\partial \eta_i}{\partial t} = F_i(t)$$
$$\frac{\partial U_i}{\partial t} = G_i(t)$$

a. Predictor

The steps of predictor method requires the use of central difference method,

$$\eta_{i,pred}^{t+\delta t} = \eta_i^{t-\delta t} + 2\delta t F_i^t$$

After all $\eta_{i,pred}^{t+\delta t}$ values are obtained, the predictor step for water particle velocity is performed,

$$U_{i,pred}^{t+\delta t} = U_i^{t-\delta t} + 2\delta t G_i^t$$

After all the values of $\eta_{i,pred}^{t+\delta t}$ dan $U_{i,pred}^{t+\delta t}$ are obtained, the corrector step is performed.

b. Corrector

Corrector is done by using numerical integration of Newton-Cote with 3 integration points (Arden, Bruce W. and Astill Kenneth N. ,1970), as follows.

$$\int_{t-\delta t}^{t+\delta t} f(t)\,dt = \delta t\left(\frac{1}{3}f^{t-\delta t} + \frac{4}{3}f^{t} + \frac{1}{3}f^{t+\delta t}\right)$$

The three-point numerical integration is formulated using a three-point Lagrange polynomial that has an accuracy

equivalent to a second-order Taylor series. The time step calculated by (19) satisfies the time step requirement where the Taylor series can be truncated to second order.

Where $\eta_{i,pred}^{t+\delta t}$ dan $U_{i,pred}^{t+\delta t}$ dihitung $F_{i,pred}^{t+\delta t}$

$$\eta_{i,cor}^{t+\delta t} = \eta_i^{t-\delta t} + \delta t\left(\frac{1}{3}F_i^{t-\delta t} + \frac{4}{3}F_i^{t} + \frac{1}{3}F_{i,pred}^{t+\delta t}\right)$$

After all the $\eta_{i,cor}^{t+\delta t}$ values are obtained, the corrector step for the water particle velocity is performed,

$$U_{i,cor}^{t+\delta t} = U_i^{t-\delta t} + \delta t\left(\frac{1}{3}G_i^{t-\delta t} + \frac{4}{3}G_i^{t} + \frac{1}{3}G_{i,pred}^{t+\delta t}\right)$$

After all values of $\eta_{i,cor}^{t+\delta t}$ dan $U_{i,cor}^{t+\delta t}$) are obtained, convergence is checked, $\left|\eta_{i,cor}^{t+\delta t} - \eta_{i,pred}^{t+\delta t}\right| < \mu$, for all points, μ being a small number. If the convergence condition is not met, the result of the corrector step becomes the predictor result, $\eta_{i,pred}^{t+\delta t} = \eta_{i,cor}^{t+\delta t}$ and $U_{i,pred}^{t+\delta t} = U_{i,cor}^{t+\delta t}$, , and the corrector step is repeated. Generally, convergence is achieved in 3 replications

VIII. MODEL OUTCOME

An assessment or evaluation of the modelled results was carried out by comparing the modelled wave profiles with the wave profiles from Wilson (1963).

8.1. Wave profile based on Wilson's criteria (1963).

The grouping of water wave profiles according to Wilson (1963) is presented in Table (6), with the profile sketched in Fig (2).

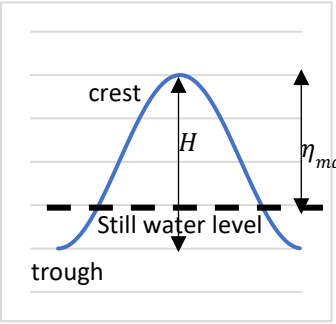

Fig (2). Wave profile based on Wilson (1963) criteria.

Table (6) Water wave profile criteria (Wilson (1963)))

Wave type	$\frac{\eta_{max}}{H}$
Airy/sinusoidal waves	< 0.505
Stoke's waves	$0.505 - 0.635$
Cnoidal waves	$0.635 - 1$
Solitary waves	$= 1$

a. Airy's Profile

The Airy wave profile is marked by its symmetrical nature, with the wave crest and trough being mirror images of each other, allowing for the wave height (H) to be approximately twice the wave amplitude (A), or $H \approx 2A$. This sinusoidal wave theory, also referred to as Airy wave theory or small amplitude wave theory, was pioneered by Airy in 1841. True to its designation, the theory is specifically tailored for waves of very small amplitudes, providing a foundational understanding of wave dynamics within this limited scope.

b. Stoke's Profile

Stokes wave theory, introduced by George Stokes in 1847, represents an advancement beyond the sinusoidal or Airy wave theory, earning it the alternative name of Finite Amplitude Wave Theory. This theory addresses some of the limitations of the Airy wave theory by accounting for waves with larger amplitudes. The distinguishing feature of the Stoke's wave profile is its asymmetry: the wave crests are sharper or steeper compared to the more gently sloped wave troughs, and it's possible for the wave profile to exhibit two distinct crests.

c. Cnoidal wave profile

The cnoidal wave theory was initially formulated by Korteweg and de Vries in 1895, upon observing the wave profile within a canal, thereby confirming its presence in natural settings. This particular wave profile is characterized by a significant disparity between the crest and the trough. Predominantly, the wave's surface is elevated above the level of still water, presenting a steep profile, whereas only a minor segment falls below, exhibiting a more gradual profile.

d. Solitary wave profile

In the case of a solitary wave profile, the entire surface of the wave remains above the level of still water. This type of wave was first identified by John Scott Russell in 1844 after he observed the phenomenon in a laboratory setting. The analytical foundation for understanding solitary waves was later established by Joseph Boussinesq in 1871. Hence, like the cnoidal wave, the solitary wave profile is also observed in natural environments.

8.2. Modeled wave profile in deep water.

The model operated at a constant water depth of $h = 30\ m$. At $x = 0$, a sinusoidal wave is introduced using the equation $\eta(0,t) = A\sin\sigma t$, where the wave period $T = 8\ sec$. This input is applied for the duration of one wave period only. The wave's amplitude is selected to match the desired wave profile. Calculations for determining the deep water depth h_0, using equations (21) and (22), categorize the 30 m water depth as deep water, as indicated in Table (7).

In the wavelength calculation results presented in Table (7), an inverse relationship is observed between wave amplitude and wavelength: as the wave amplitude

increases, the wavelength decreases. This trend contrasts with the findings.

from the numerical model, where an increase in wave amplitude results in a slightly longer wavelength. It is important to note, however, that the water depth of 30 m exceeds h_0 and thus falls into the category of deep water.

Table (7). Deep water depth h_0 measurement

A (m)	L_0 (m)	h_0 (m)
0.02	21.288	19.149
0.5	19.643	17.429
1.3	15.849	13.614

For the execution of this numerical model, a deep water coefficient $\theta = 1.8$. is employed. Additionally, a range for the weighting coefficient $\varepsilon = 0.015 - 0.035$ is used, where a larger wave amplitude corresponds to a higher value of ε the weighting coefficients are detailed in Table (1). The model runs over eight wave periods, equivalent to 80 seconds. During the initial two wave periods, the wave profile undergoes an evolution, rendering it unstable. From the third wave period onward, the wave profile achieves stability.

a. Sinusoidal profile

With input wave amplitude $A = 0.02\ m$, $\frac{\eta_{max}}{H} = \frac{0.02}{0.04} = 0.5$ is obtained (Fig(3)). This condition corresponds to Wilson's criterion for sinusoidal wave profile.

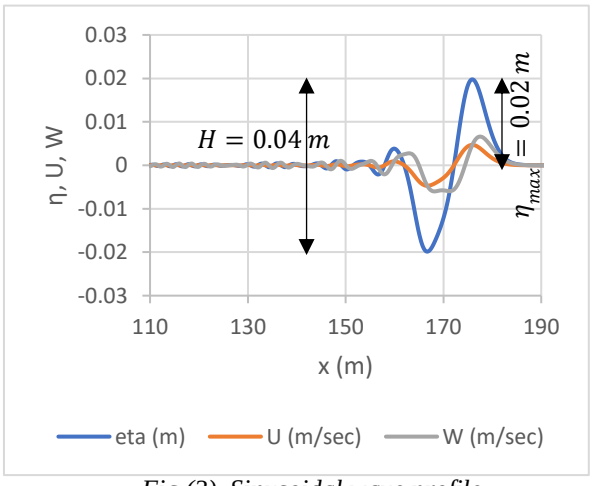

Fig (3). Sinusoidal wave profile

b. Stoke's wave Profile

Stoke's profile, obtained using $A = 0.5\ m$. The modelled results can be seen in Fig (4). $\frac{\eta_{max}}{H} = \frac{0.605}{1.0} = 0.605$ is obtained, this condition is in accordance with Wilson's criteria for Stoke's wave profile.

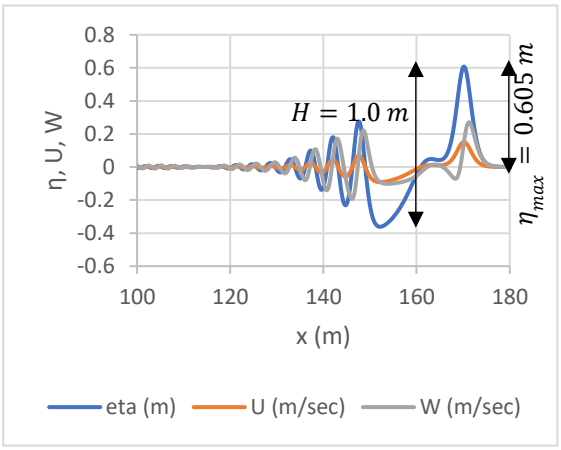

Fig (4). Stoke's profile

c. Cnoidal wave Profile

The model was executed with an input of $A = 1.30\ m$, or $H = 2.60$ m. This is the largest wave height for a wave period of 8 sec. $\frac{\eta_{max}}{H} = \frac{2.1}{2.6} = 0.808$ was obtained, in accordance with Wilson's criteria, for a Cnoidal profile. The image of this cnoidal profile is presented in Fig (5).

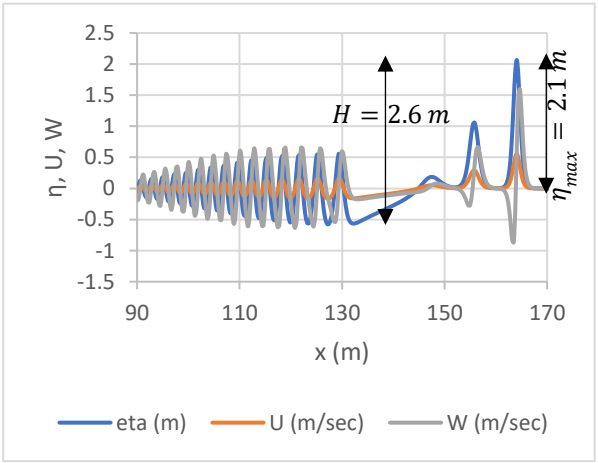

Fig (5). Cnoidal profile

In this section, it was found that the model execution in deep water did not obtain a solitary wave profile, even though the maximum wave amplitude was used.

8.3. The Effect of water depth on wave profile.

In this section, the effect of water depth on wave profiles is explored using a model that simulates a sinusoidal wave input at $x = 0.0$ expressed as $\eta(0,t) = A \sin \sigma t$, which is applied for the duration of a single wave period of 12.0 seconds. The model uses a wave amplitude of 2.0 meters, equivalent to a wave height $H = 4.0\ m$. For this scenario, the deep water depth h_0 is calculated to be 41.0 meters. The experiment is conducted at water depths of 41.0 meters, 20 meters, and 8.0 meters to observe the resulting wave profiles. At the depth of 41.0 meters, matching the deep water depth h_0, the model produces a Stoke's wave profile,

depicted in Fig (6). When executed at a water depth of 20 meters, the model forms a cnoidal wave profile, as shown in Fig (7) and in a water depth 8.0 m, solitary wave profile was obtained (Fig.(8)).

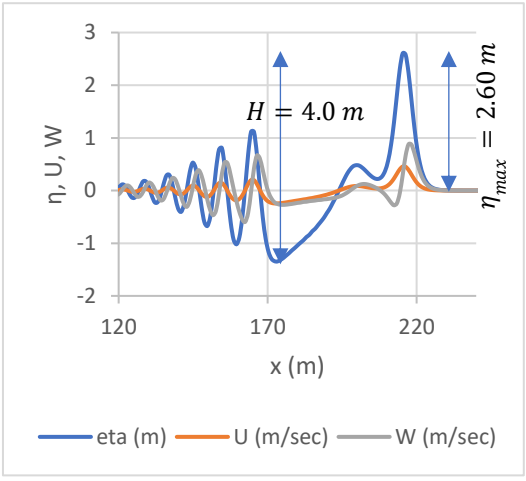

Fig (6).Stoke's profile $\frac{\eta_{max}}{H} = 0.6$

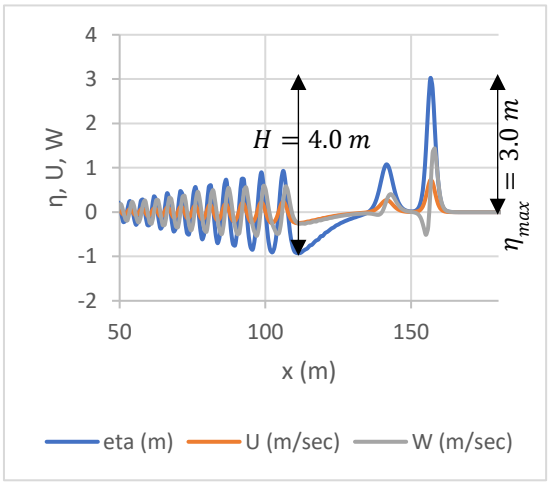

Fig (7).Cnoidal profile $\frac{\eta_{max}}{H} = 0.75$

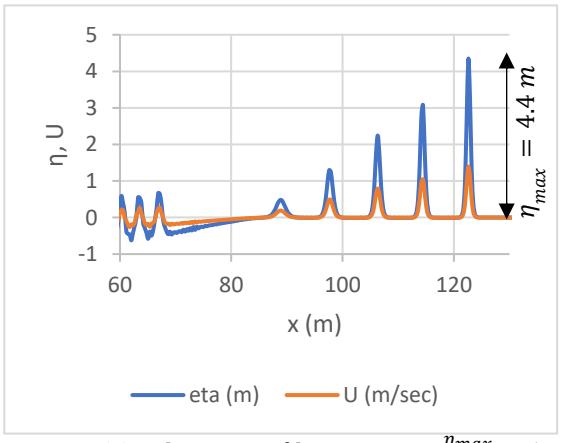

Fig (8).Solitairy profile $\eta_{max} = H, \frac{\eta_{max}}{H} = 1$

In the observed solitary wave profile, an increase in wave height is noted, from the initial 4.0 meters (input) to 4.40 meters. This increase is believed to be a result of the wave setup phenomenon, which is characteristic of shallow water effects. According to Wilson's criterion for solitary waves, the ratio of the maximum wave height $\frac{\eta_{max}}{H} = 1$. However, the wave trough is not considered in this analysis due to its minimal size and the presence of numerous other wave crests.

8.4. Model execution at the sloping bottom.

In a subsequent experiment, the model is applied to a canal featuring an upstream water depth of 15.0 meters and a downstream depth of 5.0 meters, with the channel extending over a length of 200.0 meters. The input for this setup is a sinusoidal wave characterized by a wave period of 8.0 seconds and a wave amplitude of 0.50 meters. The outcomes of this experiment are depicted in Fig (9), illustrating that at a water depth of 6.0 meters, the wave undergoes shoaling, which results in the wave height increasing to 1.40 meters and the wave adopting a solitary profile.

The results from executing the model reveal its capability to simulate various wave profiles, including sinusoidal, Stoke's, cnoidal, and solitary profiles. Importantly, the formation of these profiles is influenced not only by the wave amplitude but also significantly by water depth, particularly in the case of the solitary profile. An amplitude that results in a Stoke's profile in deep water conditions may lead to a cnoidal profile in shallower waters, and similarly, the same amplitude can generate a solitary profile in even shallower depths. This underscores the critical role that both water depth and wavelength play in determining the specific wave profile that emerges.

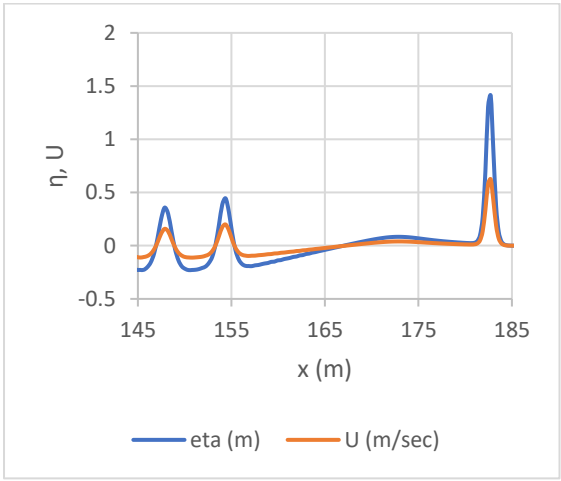

Fig (9). Solitary wave profil due to shoaling.

The occurrence of a solitary profile in shallow water suggests that the model's wavelength is sufficiently short

to facilitate the formation of such a profile. The weighting coefficient emerges as a crucial parameter in shaping the wavelength, indicating that this coefficient, as part of the weighted Taylor series, significantly influences the outcomes of the model. This observation highlights the interconnectedness of wave amplitude, water depth, wavelength, and model parameters like the weighting coefficient in the complex dynamics of wave profile formation.

IX. CONCLUSION

The study reveals that the time series model developed can generate wave profiles aligning with previous research, notably including the cnoidal and solitary wave profiles. This demonstrates the model's capability to effectively simulate water waves.

The solitary wave profile emerges at short wavelengths, where the model's wavelength determination hinges on the weighting coefficients within the weighted Taylor series. This suggests the selected weighting coefficients are well-suited for the task.

Moreover, the model's performance is influenced by the chosen time step and grid size. These parameters are aligned with the foundational hydrodynamics equations' assumptions, which presuppose truncation of the Taylor series to first order. Additionally, the time step and grid size adhere to the Finite Difference Method's requirements, where the Taylor series truncation is limited to the second order, ensuring a comparable level of numerical integration accuracy. The coherence between the time step and grid size also meets Courant's criteria, further validating the model's configuration.

In summary, the employment of a weighted Taylor series to formulate the time series model, coupled with the strategic selection of time step and grid size for numerical solution, leads to robust model outcomes.

REFERENCES

[1] Hutahaean, S. (2023a). Method for Determining Weighting Coefficients in Weighted Taylor Series Applied to Water Wave Modeling. International Journal of Advance Engineering Research and Science (IJAERS). Vol. 10, Issue 12; Dec, 2023, pp 105-114. Article DOI: https://dx.doi..org/10.22161/ijaers.1012.11.

[2] Dean, R.G., Dalrymple, R.A. (1991). Water wave mechanics for engineers and scientists. Advance Series on Ocean Engineering.2. Singapore: World Scientific. ISBN 978-981-02-0420-4. OCLC 22907242.

[3] Arden, Bruce W. and Astill Kenneth N. (1970). Numerical Algorithms : Origins and Applcations. Philippines copyright (1970) by Addison-Wesley Publishing Company, Inc.

[4] Hutahaean, S. (2023b). Water Wave Velocity Potential on Sloping Bottom in Water Wave Transformation Modeling . International Journal of Advance Engineering Research and Science (IJAERS). Vol. 10, Issue 10; Oct, 2023, pp 149-157. Article DOI: https://dx.doi..org/10.22161/ijaers.1010.15.

[5] Hutahaean, S. (2024). Breaking Index Study on Weighted Laplace Equation. International Journal of Advance Engineering Research and Science (IJAERS). Vol. 11, Issue 1; Jan, 2024, pp 34-43. Article DOI: https://dx.doi..org/10.22161/ijaers.11.6.

[6] Protter, Murray, H.; Morrey, Charles, B. Jr. (1985). Differentiation Under The Integral Sign. Intermediate Calculus (second ed.). New York: Springer pp. 421-426. ISBN 978-0-387-96058-6.

[7] Courrant, R., Friedrichs, K., Lewy, H. (1928). Uber die Pertiellen Differenzengleic hungen der mathematiscen Physik. Mathematiscen Annalen (in German). 100 (1);32-74, Bibcode : 1928, MatAn. 100.32.c. doi: 10.1007/BF01448839, JFM 54.0486.01 MR 1512478.

[8] Arden, Bruce W. and Astill Kenneth N. (1970). Numerical Algorithms : Origins and Applcations. Philippines copyright (1970) by Addison-Wesley Publishing Company, Inc.

[9] Wilson, B.W. (1963). Condition of Existence for Types of Tsunami Waves, paper presented at XIIIth Assembly IUGG, Berkeley, California, August 1963 (unpublish).

[10] Airy, G.B. (1841). Tides and waves. In Hughs James Rose: et.al (eds.) Encyclopedia Metropolitana. Mixed Science. Vol.3 (published 1817-1845). Also: Trigonometry, On the Figure of the Earth, Tides and Waves. 396 pp.

[11] Stokes, G.G. (1847). On the Theory of Oscillatory Waves.Trans Camb. Phil.Soc., Vol.8 pp.441-455. Also Math Phys. Papers, Vol. 1, Camb. Univ. Press, 1880.

[12] Korteweg, D.J. and De Vries, J. (1895). On the Change of Form of Longwaves Advancing, in a Rectangular Canal, and on a New Type of Long stationary Waves. Phil.Mag., 5th Series, Vol. 39, pp. 422-443.

[13] Russel, J.S., 1844. Report on Waves. 14th Meeting Brit. Assoc. Adv. Sci., pp. 311-390.

[14] Boussinesq, J. , 1871. Theori de L'intumesence Liquide , Apelee Onde Solitaire ou de Translation se Propageant Dans un Canal Rectangulaire. Comptes Rendus Acad . Sci., Paris, Vol.72, pp.755-759.